A Novel MPPT Algorithm for Dual-Inverter Grid-Connected PV Applications

Gabriele Grandi, Darko Ostojic, and Claudio Rossi
DEPARTMENT OF ELECTRICAL ENGINEERING
UNIVERSITY OF BOLOGNA
Tel.: +39 / 051-2093571.
Fax: +39 / 051-2093588.
E-Mail: <name.surname>@mail.ing.unibo.it
URL: http://www.die.unibo.it

Keywords

Photovoltaic, Power conditioning, Voltage Source Inverters, Multilevel converters.

Abstract

A novel MPPT algorithm for three-phase grid-connected photovoltaic generation systems is presented in this paper. Reference is made to a conversion scheme consisting in two balanced arrays of PV modules, each one feeding a standard 2-level three-phase voltage source inverter (VSI). The dc-link voltages of each VSI are regulated according with the requirement of the proposed MPPT algorithm, based on the comparison of the operating points of the two PV arrays. Inverters are connected to grid by a three-phase transformer with open-end windings configuration on inverters side. The resulting conversion structure performs as a power active filter, doubling the power capability of a single VSI, with the additional benefit of multilevel voltage waveforms. The proposed MPPT algorithm has been successfully verified by experimental tests.

Introduction

The connection of PV fields to the ac grid is usually made with a voltage source inverter (VSI), and it may include intermediate dc/dc chopper, transformer, or even both [1]. In many countries the national electric code requires a transformer to achieve galvanic insulation of PV modules with respect to the grid [2]. The presence of a dc/dc chopper allows the PV field to operate over a wider voltage range, with a fixed inverter dc voltage and a simplified system design. On the other hand, the dc/dc chopper increases the cost and decreases the conversion efficiency at most operating points. Transformerless and high-frequency transformer topologies are preferred for omitting bulky LF transformer, but limited to single-phase output with powers up to few kW. The restrictions arise from switching losses and limited power of the HF magnetic components. Hence, PV conversion schemes including a line-frequency transformer are prevailing in higher power range, i.e., from few tens of kW up to MW, also because the cost per watt of LF transformer decreases as rated power increases.
Maximum power point trackers (MPPT) act in order to force the operating point of PV modules on their peak power. There are many studies dealing with MPPT and introducing different strategies for following the peak power point [3], such as the “perturbation and observation” method (P&O) [4], the “incremental conductance” method, [5], and the “ripple correlation control” [6]-[8]. More recently, further methods have been proposed such as “pilot-cell” method [9], “fuzzy control” [10] etc.
In this paper, the dual VSI topology presented by the Authors in [11], [12] is considered, and a novel MPPT algorithm has been applied to maximize power injection into the grid, according to the block diagram of Fig. 1. The two standard 2-level VSI are connected to open-end primary windings of a standard three-phase transformer. The whole PV field is shared into two equal PV arrays. Each inverter is directly wired with one of the PV arrays. The secondary windings are connected to the grid with a traditional star (or delta) configuration. Note that the transformer contributes with its leakage inductance to the ac-link inductance which is always necessary for the grid coupling of a VSI. Furthermore, the presence of a low-frequency transformer enable the direct connection of high power

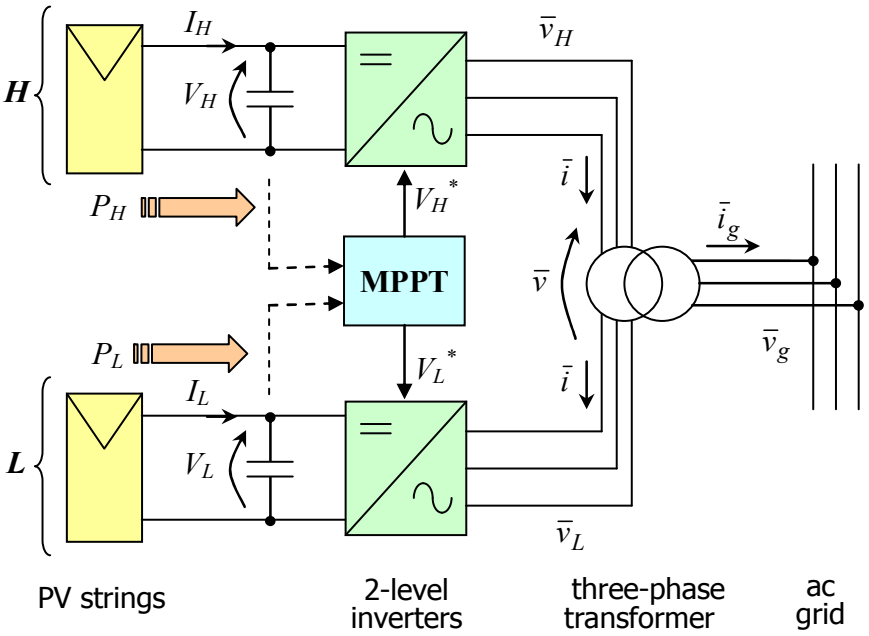

Fig. 1: Block diagram of the dual VSI topology including an open-winding three-phase transformer.

generation systems to either medium- or high-voltage grids (10 kV or more). The resulting three-phase converter is able to operate as a voltage multilevel inverter, equivalent to a 3-level inverter, with reduced harmonic distortion and lower *dv*/*dt* in the output voltages.
The MPPT algorithm proposed in this paper is based on a forced small displacement in the working points of the two PV arrays, allowing sharing of data between them on the basis of instantaneous currents measurement. Similar MPPT schemes have been recently presented in [13] and [14], but with reference to different PV conversion structures. A control algorithm with standard PI controllers is adopted to achieve commanded values of dc voltages necessary for the MPPT regulation of PV arrays. For this purpose, an improved space vector modulation strategy has been developed to provide proper voltage multilevel output waveforms and simple implementation on a standard DSP.

The dual VSI topology

Three-level inverters are a good tradeoff solution between performance and cost in multi-level converter for both medium and high-power applications. In particular, the output phase voltage waveform of the converter has up to nine levels. The dual 2-level inverter structure (Fig. 1) gives the same output voltage as 3-level inverter with a simple combination of standard three-phase VSI [15], [16]. Then, it represents a viable solution when the three-phase output can be connected in the open-winding configuration, as for transformers and ac motors, and especially when the dc source can be easily split in two insulated supplies, as for batteries and PV fields. The presence of two insulated dc sources easily prevents the circulation of common-mode currents, avoiding the use of an additional three-phase mode reactor. An alternative solution in case of a single dc source consists in the application of a modified voltage modulation algorithm which doesn't produce common-mode voltages, but with the drawback of a lower dc bus voltage utilization [17].
In the present case of PV applications, the proper dc voltage range can be obtained by adjusting the number of series-connected modules for each PV array (string), avoiding the use of intermediate dc/dc choppers. In this case, inverters regulate dc-bus voltages according to the MPPT requirements, as explained in the following section.
With reference to the scheme of Fig. 1, using space vector representation, the output voltage vector $\bar{v}$ of the multilevel converter is given by the contribution of the voltage vectors $\bar{v}_H$ and $\bar{v}_L$ generated by inverter *H* and *L*, respectively [16],

$$\bar{v} = \bar{v}_H + \bar{v}_L \,. \tag{1}$$

 ISBN: 9789075815009

Dc voltage controller

The conversion system is symmetric, having both inverters with equal ratings and two equal groups (arrays) of PV modules supplying them. The dc bus voltage references generated by the MPPT controller, V_H^* and V_L^*, are very close one to the other, as discussed in the next section. Two distinct voltage controllers have been implemented, according with the block diagram shown in Fig. 2. In particular, the two dc voltages (V_H, V_L) are regulated by two controllers, here called "sigma" (Σ) and "delta" (Δ). The voltage controller Σ acts in order to regulate the average value of dc bus voltages, V_{dc} (i.e., their sum), whereas the voltage controller Δ acts in order to set the difference between the dc bus voltages (ΔV). The input signals of both voltage controllers, V_Σ and V_Δ, can be built by adding and subtracting one from the other the individual dc voltage errors ΔV_H and ΔV_L, as follows

$$V_\Sigma = \Delta V_H + \Delta V_L = (V_H + V_L) - (V_H^* + V_L^*), \tag{2}$$

$$V_\Delta = \Delta V_H - \Delta V_L = (V_H - V_L) - (V_H^* - V_L^*), \tag{3}$$

being:

$$\begin{cases} \Delta V_L = V_L - V_L^* \\ \Delta V_H = V_H - V_H^* \end{cases}. \tag{4}$$

Ac current controller

The voltage controller Σ directly generates the current reference for the dual inverter, I^*, corresponding to the active power injected into the grid, regardless to the power sharing between the two inverters "H" and "L", as shown in Fig. 2. If the ac current is in phase with the grid voltage, the resulting current space vector reference $\bar{i}^*$ is

$$\bar{i}^* = I^* \hat{v}_g, \tag{5}$$

being $\hat{v}_g$ the unity space vector of the grid voltage. It can be noted that reactive and/or harmonic compensation current references can be added to $\bar{i}^*$ if active power filter operation is required.
To solve the known problem of current control in grid-connected application [18], a simple proportional controller with a feed-forward action (grid voltage) has been adopted, due to its simplicity, good dynamic response and immunity to harmonic disturbance. In particular, the reference voltage $\bar{v}^*$ is calculated as

$$\bar{v}^* = K_c(\bar{i}^* - \bar{i}) + \bar{v}_g', \tag{6}$$

being $\bar{v}_g'$ the space vector of the grid voltage at the inverter side.

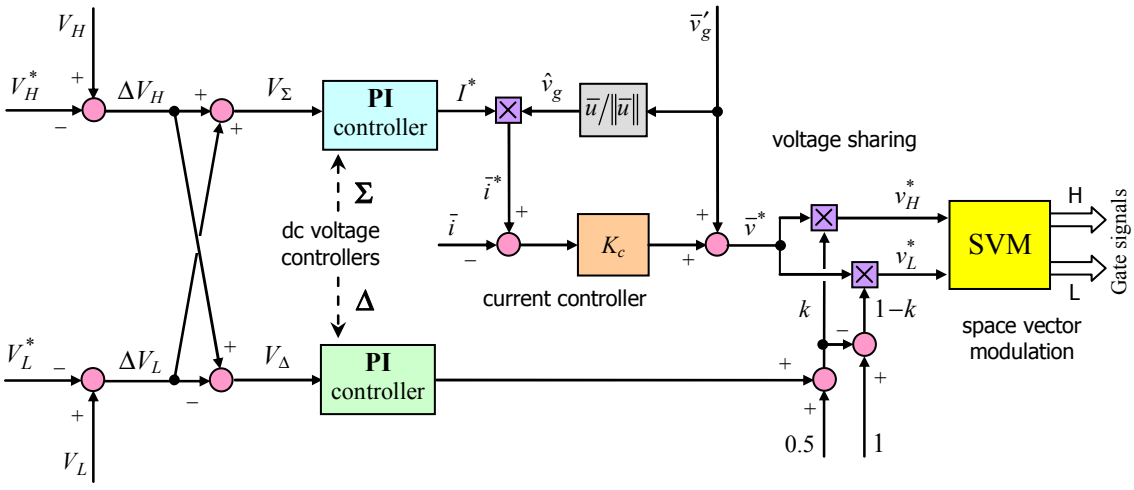

Fig. 2: Schematic diagram of proposed control system.

Voltage and power sharing

The reference output voltage $\bar{v}^*$ calculated by (6) can be synthesized as the sum of the voltages $\bar{v}_H^*$ and $\bar{v}_L^*$ generated by the two inverters, as expressed by (1). In order to equalize the two dc bus voltages V_H and V_L, the PI-controller Δ determines the power sharing between the two inverters "H" and "L", as shown in Fig. 2. Introducing the voltage ratio k and imposing the inverter voltage vectors $\bar{v}_H^*$ and $\bar{v}_L^*$ to be in phase with the output voltage vector $\bar{v}^*$, yields

$$\begin{cases} \bar{v}_H^* = k\,\bar{v}^* \\ \bar{v}_L^* = (1-k)\,\bar{v}^* \end{cases}, \tag{7}$$

The condition expressed by (7) allows maximum dc voltage utilization. Being the output current of the two inverters the same, the coefficient k also defines the power sharing between the two inverters. In terms of averaged values within the switching period, the output power can be expressed as

$$p = \frac{3}{2}\bar{v}^* \cdot \bar{i} = p_H + p_L\,, \tag{8}$$

where p_H and p_L are the individual powers from the two inverters. By combining (8) with (7) leads to

$$p_H = \frac{3}{2}\bar{v}_H^* \cdot \bar{i} \;\; = k\,p\,, \tag{9}$$

$$p_L = \frac{3}{2}\bar{v}_L^* \cdot \bar{i} \;\; = (1-k)\,p\,. \tag{10}$$

The coefficient k has a limited variation range depending on the value of the reference output voltage, $\bar{v}^*$, as already investigated by the Authors in [16]. Furthermore, it has to be verified that both references are within the range of achievable output voltages of each inverter, which depend on their dc voltages. In the case of a single inverter topology, if the voltage demand exceeds available dc voltage, the output voltage is simply saturated. With the dual inverter configuration, total voltage reference must be satisfied, so in case of voltage saturation of one inverter the second has to provide for the missing part. This problem was addressed in [11].

Once the inverter reference voltages $\bar{v}_H^*$ and $\bar{v}_L^*$ are determined by (7), they must be synthesized by the dual two-level inverter and applied to the open-end windings of the transformer. A SVM providing proper voltage multilevel waveforms have been presented in [16]. However, this method leads to switching sequences that are difficult to be implemented in the sole PWM generation unit of an industrial DSP which usually provides a unique carrier for all three phases. For this reason, the Authors presented a modified SVM algorithm in [19], more suitable for an implementation. It introduces use of asymmetrical PWM in order to avoid application of different carriers, as mentioned above. This new algorithm has been adopted here.

Proposed MPPT algorithm

The well-known problem of the maximum power point tracking consists in finding the MPP voltage, V_{MPP} (or the MPP current, I_{MPP}), at which the PV field provides the maximum output power, P_{MPP}. MPP continuously moves, according to variations in environmental conditions (i.e. solar irradiation and cell temperature). Among the numerous known solutions [3]-[10], one is particularly suitable for the dual inverter configuration, due to the presence of two identical groups of PV modules [13], [14]. The algorithm is based on deliberate introduction of a small difference ΔV^* (in the order of %) between reference voltages of the two PV fields V_H^* and V_L^*, as follows

$$V_L^* = K_v\,V_H^*\,, \tag{11}$$

$$\Delta V^* = V_H^* - V_L^* = (1-K_v)\,V_H^*\,, \tag{12}$$

 ISBN: 9789075815009

where the coefficient K_v slightly differs from 1 ($k \cong 0.95 \div 0.98$). Due to the particular shape of power vs. voltage characteristic (P-V curve), the powers generated by the two PV fields, P_L and P_H, practically coincide if the operating points are on the "flat" in neighborhood of MPP, according to Fig. 3. Conversely, on "sloped" parts of the P-V curve, one of the powers is higher than the other, or vice-versa, depending on the position of the operating points with respect to the MPP. In particular, the following three possibilities occur:

$$\begin{cases} P_L < P_H \;\Rightarrow\; V < V_{MPP} \\ P_L = P_H \;\Rightarrow\; V \cong V_{MPP} \\ P_L > P_H \;\Rightarrow\; V > V_{MPP} \end{cases} \tag{13}$$

In effect, the difference between P_H and P_L gives an estimation of the slope of the P-V characteristic:

$$\frac{dP}{dV} \cong \frac{P_H - P_L}{(1-K_v)V_H} \cong K_p\left(P_H - P_L\right), \tag{14}$$

Hence, reference dc voltages V_H^* and V_L^* can be found as the output of a simple PI-controller acting on the error between the two powers, as represented in Fig. 3.
The choice of a proper value for K_v is a tradeoff between efficiency, which is higher as K_v approaches 1, and immunity to both noise and PV modules asymmetry, which increase as K_v diverge from 1. Obviously, the proposed algorithm is based on the assumption that the two PV arrays have the same P-V (or I-V) characteristic. For this reason, the PV arrays should consist of equal number and same type of PV modules. In spite of *P-V* characteristics of two identical PV modules slightly differ one from the other (the dispersion is in the order of few %), when many PV modules are arranged in two big arrays, their global P-V characteristics are averaged and practically coincides.
On the basis of (2) and (3), the effects of PI regulators Σ and Δ lead to the following steady-state conditions

$$V_\Sigma = 0 \;\Rightarrow\; V_H + V_L = V_H^* + V_L^*, \tag{15}$$

$$V_\Delta = 0 \;\Rightarrow\; V_H - V_L = \Delta V^*. \tag{16}$$

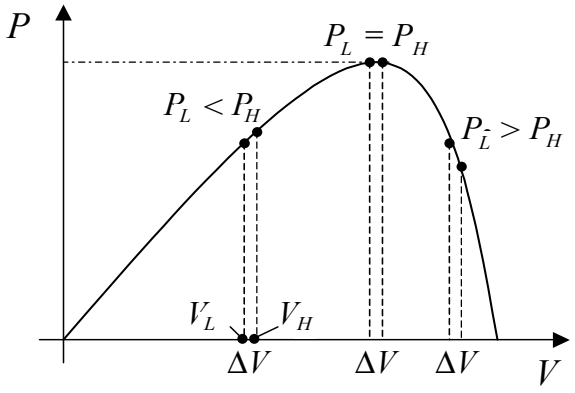

(a) P-V diagram

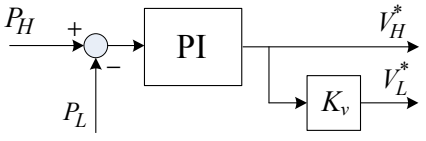

(b) Control scheme

Fig. 3: Principle of MPPT algorithm.

Implementation and experimental results

To ensure the safety, the system has been implemented by using only parallel connections of PV modules, since the presence of a grid-transformer with the proper turn ratio enables voltage adaptation. The resulting PV array voltage range is the same of a single PV module, in the range 20÷40 V, allowing use of low-voltage MOSFETs. These types of switches are cheap, being widely used in automotive applications, and they feature good efficiency, since MOSFETs on-state resistance is a strong decreasing function of the blocking voltage rating. The main characteristics of the whole PV generation system prototype are summarized in Table I, and some pictures of the experimental set-up are given in Fig. 4. Reference is made to the scheme presented in Fig. 1, with the PV module arrays consisting in six PV modules in parallel, directly connected to the inverters. In this case, the MPPT regulation is achieved by adjusting the dc bus voltage references V_L^* and V_H^* of the two inverters, according with the proposed algorithm.
The experimental results show the action of the MPPT controller with reference to opposite starting conditions and with different values of the MPPT parameters.
Figs. 5 and 6 are related to the case of a coefficient K_v = 0.96, leading to a difference between V_H and V_L of about 1 V. In particular, Fig. 5 (a) shows the time behaviour of dc voltage, dc current, and power for both the inverters starting from the open-circuit voltage (around 35-40 V) to the MPP, whereas Fig. 5 (b) shows the same transient on the corresponding P-V diagram. It can be noted that steady state is reached in about 100 ms, with a smoothed oscillation around the MPP. The same variables are presented in Fig. 6 with reference to a transient from the minimum dc voltage (around 20-25 V) to the MPP. In this case, the voltage excursion is lower, and the settling time is halved (about 50 ms), without oscillations.

Table I: Main parameters of the experimental setup

Each of the 2 PV arrays: 6 x Shell Solar SQ150-C (in parallel)				
Grid transformer			Three-Phase Inverter (2x)	
single-phase, 50 Hz	3x		IRF2807 (parallel MOSFETs)	6x
rated voltages (V)	24/400		rated dc voltage (V)	50
rated power (VA)	500		rated ac current (A)	240
short circuit voltage (%)	6.9		switching freq. (kHz)	20
ac-link inductance (mH)	0.4		dc-bus capacitance (mF)	26

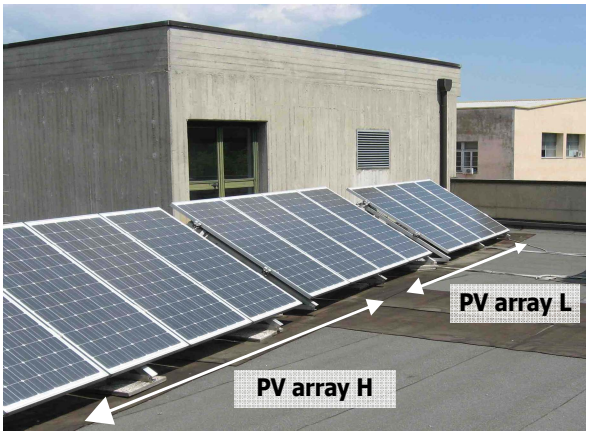

(a) Arrangement of 6+6 PV modules on the roof.

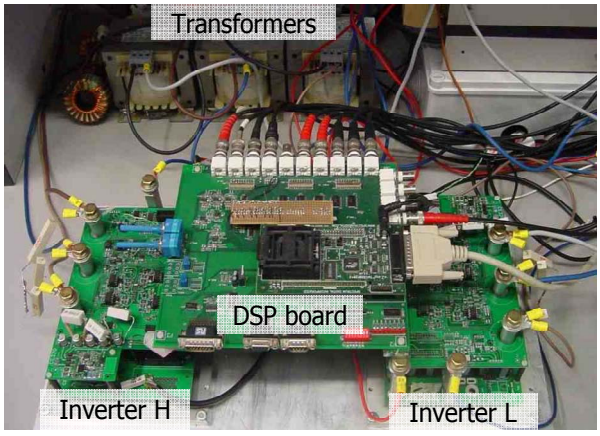

(b) Dual two-level converter in the Lab.

Fig. 4: Pictures of the experimental setup.

 ISBN: 9789075815009

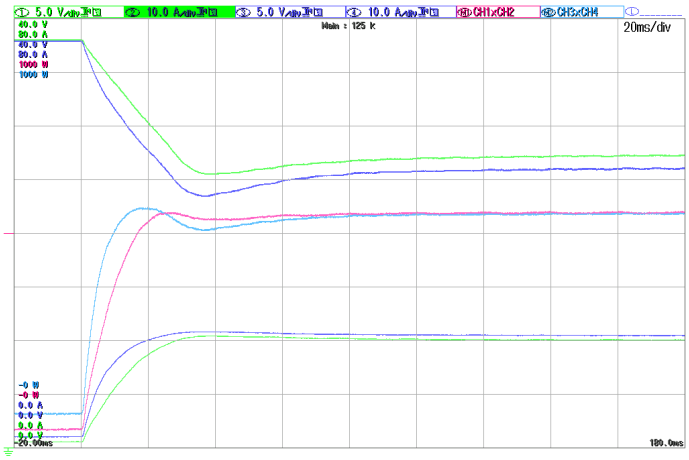

(a) V_H, V_L (5 V/div, top), P_L, P_H (125 W/div, middle), I_L, I_H (10 A/div, bottom).

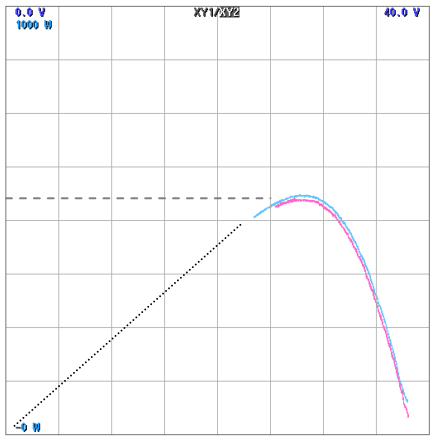

(b) P_L vs. V_L and P_H vs. V_H (5 V/div, 125 W/div).

Fig. 5: Experimental results: transient from no-load to MPP with $K_v = 0.96$.

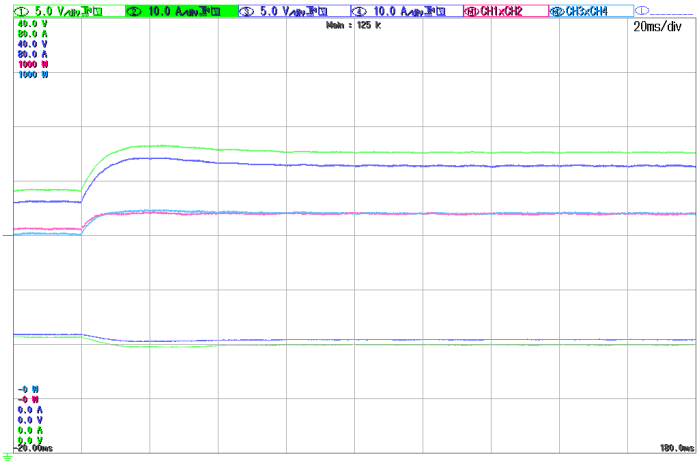

(a) V_H, V_L (5 V/div, top), P_L, P_H (125 W/div, middle), I_L, I_H (10 A/div, bottom).

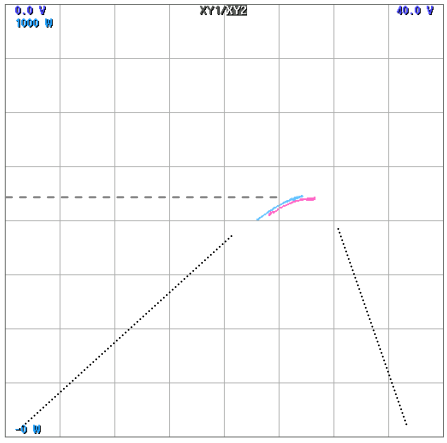

(b) P_L vs. V_L and P_H vs. V_H (5 V/div, 125 W/div).

Fig. 6: Experimental results: transient from minimum dc voltage to MPP with $K_v = 0.96$.

Figs. 7 and 8 are related to the case of a coefficient $K_v = 0.98$, leading to a reduced difference between V_H and V_L, about 0.5 V. Also in this case, the former diagrams, Fig. 7, show the transient to the MPP starting from the open-circuit voltage, whereas the latter diagrams, Fig. 8, show the transient to the MPP starting form the minimum dc voltage. Steady-states and settling times are very close to the previous case with $K_v = 0.96$, proving that also with a very small voltage displacement a satisfactory behaviour of the MPPT algorithm can be obtained.
Figs. 9 and 10 correspond to the same cases shown in Figs. 7 and 8, respectively, by adjusting the PI parameters in order to avoid oscillations around the MPP. In particular, Fig. 9 shows that, despite of the large voltage excursion between open-circuit and MPP, the steady-state condition is reached without oscillations in about 40 ms.
Note that, in all the examined cases, both the steady-state powers P_H and P_L practically coincide with the MPP, proving the effectiveness of the proposed MPPT algorithm.

 ISBN: 9789075815009

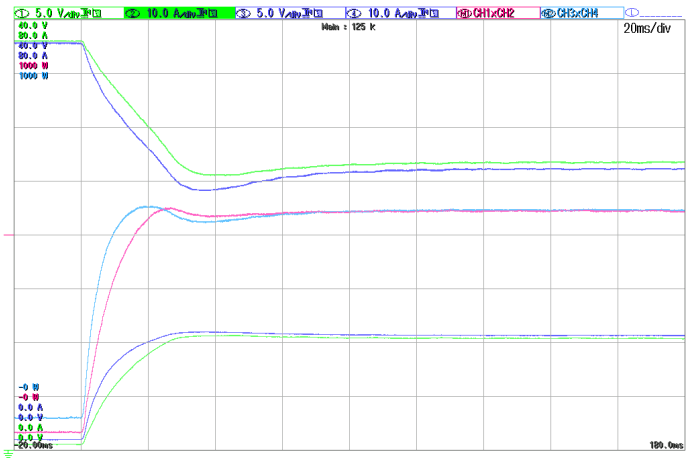

(a) V_H, V_L (5 V/div, top), P_L, P_H (125 W/div, middle), I_L, I_H (10 A/div, bottom).

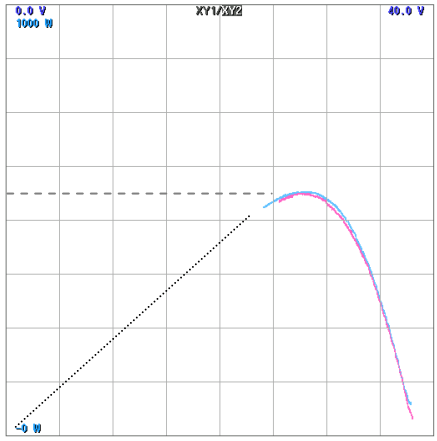

(b) P_L vs. V_L and P_H vs. V_H (5 V/div, 125 W/div).

Fig. 7: Experimental results: transient from no-load to MPP with $K_v = 0.98$.

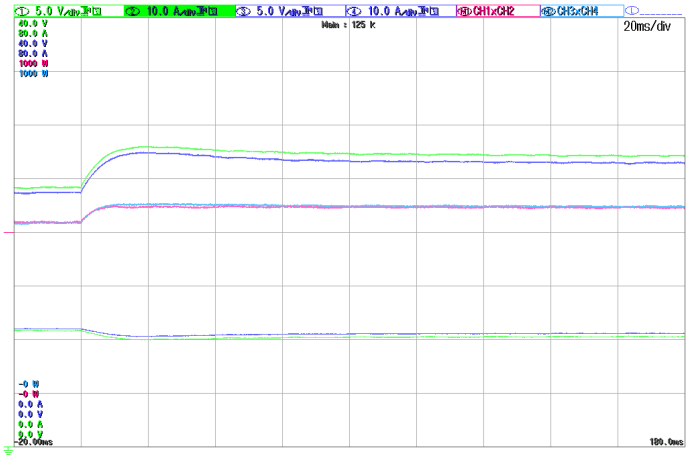

(a) V_H, V_L (5 V/div, top), P_L, P_H (125 W/div, middle), I_L, I_H (10 A/div, bottom).

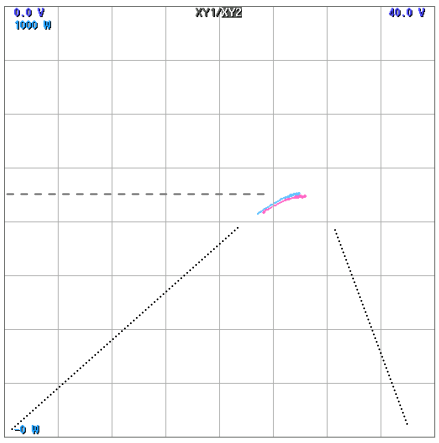

(b) P_L vs. V_L and P_H vs. V_H (5 V/div, 125 W/div).

Fig. 8: Experimental results: transient from minimum dc voltage to MPP with $K_v = 0.98$.

Conclusion

In this paper a new MPPT algorithm has been proposed, suitable for dual-inverter grid-connected PV generation systems. The conversion scheme acts as a power conditioner, with the same voltage multi-level waveforms as a 3-level VSI. The voltages of the two identical PV arrays supplying the two standard 2-level VSIs are regulated according with the MPP controller, based on the comparison of the operating points of the two PV arrays. The proposed MPPT algorithm has been successfully implemented and experimental results are given in the paper with reference to different cases. In particular, the experimental tests show that MPP can be reached in few tens of milliseconds starting from both the open-circuit voltage and the minimum operating voltage. Furthermore, the voltage displacement between the two PV arrays can be reduced to few percents, leading to operating points practically coinciding with the MPP, without an appreciable loss of conversion efficiency.

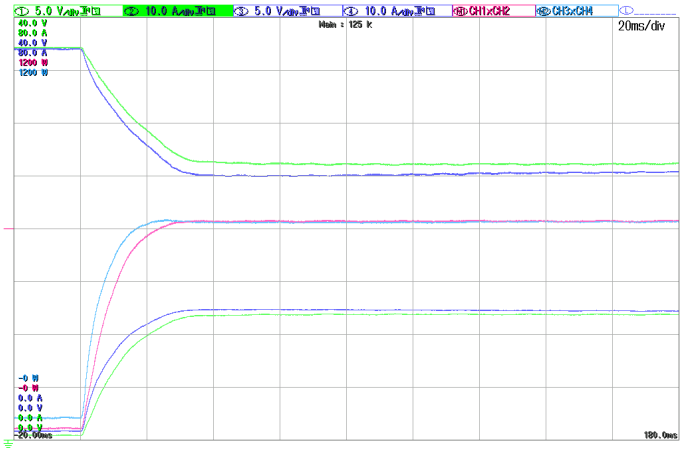

(a) V_H, V_L (5 V/div, top), P_L, P_H (150 W/div, middle), I_L, I_H (10 A/div, bottom).

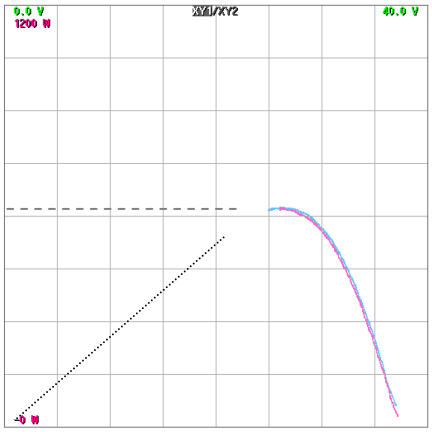

(b) P_L vs. V_L and P_H vs. V_H (5 V/div, 150 W/div).

Fig. 9: Experimental results: transient from no-load to MPP with K_v = 0.98.

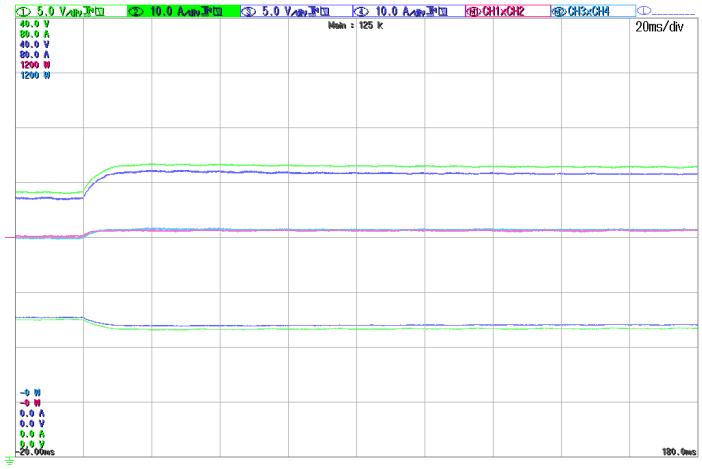

(a) V_H, V_L (5 V/div, top), P_L, P_H (150 W/div, middle), I_L, I_H (10 A/div, bottom).

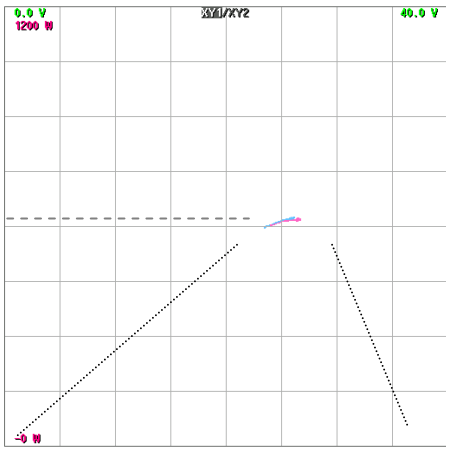

(b) P_L vs. V_L and P_H vs. V_H (5 V/div, 150 W/div).

Fig. 10: Experimental results: transient from minimum dc voltage to MPP with K_v = 0.98.

References

[1] Kjaer, J. Pedersen, F. Blaabjerg: A Review of Single-Phase Grid-Connected Inverters for Photovoltaic Modules, IEEE Trans. Industry Applications, Vol. 41, No. 5, Sep 2005, pp. 1292-1306.

[2] F. Schimpf, L. Norum: Grid Connected Converters for Photovoltaic, State of the Art, Ideas for Improvement of Transformerless Inverters, Nordic Workshop on Power and Industrial Electronics NORPIE 2008, Espoo, Finland, 9-11 June 2008.

[3] Chihchiang Hua, Chihming Shen: Comparative study of peak power tracking techniques, Proc. of IEEE Applied Power Electronics Conference, APEC, 1998, Vol.2., pp. 679-685.

[4] J. H. R. Enslin and D.B. Snyman: Simplified feed-forward control of the maximum power point tracker for photovoltaic applications, Proc. of IEEE Power Electronics Motion Control Conference, IECON, 1992, Vol. 1, pp. 548-553.

[5] M. Bodur, M. Ermis: Maximum power point tracking for low power photovoltaic solar modules, Proc. of 7th IEEE Mediterranean Electrotechnical Conference, MELECON, 1994, Vol. 2. pp. 758-761.

[6] T. Esram, J. Kimball, P. Krein, P. Chapman, P. Midya: Dynamic Maximum Power Point Tracking of Photovoltaic Arrays Using Ripple Correlation Control, IEEE Trans. Power Electronics, Vol. 21, No. 5, Sep. 2006, pp. 1282- 1291.

[7] G. Grandi, D. Casadei, C. Rossi: Direct coupling of power active filters with photovoltaic generation systems with improved MPPT capability, IEEE PowerTech Conf, Bologna (Italy), June 23-26, 2003.

[8] D. Casadei, G. Grandi, C. Rossi: Single-phase single-stage photovoltaic generation system based on a ripple correlation control maximum power point tracking, IEEE Trans. on Energy conversion, Vol. 21 No. 2, June 2006, pp. 562-568.

[9] G.W. Hart, H.M. Branz, C.H. Cox: Experimental tests of open loop maximum power point tracking techniques for photovoltaic arrays, Solar Cells, Vol. 13, 1984, pp. 185-195.

[10] M. Veerachary, T. Senjyu, K. Uezato: Feedforward maximum power point tracking of pv systems using fuzzy controller, IEEE Trans. on Aerospace and Electronic Systems, Vol. 38, No. 3, July 2002, pp. 969-981.

[11] G. Grandi, D. Ostojic, C. Rossi: Dual Inverter Configuration for Grid-Connected Photovoltaic Generation Systems, Proc. 29th Int. Tel. En. Conf., INTELEC, Sept. 30 –Oct. 4, 2007, Rome, Italy, pp. 880-885.

[12] G. Grandi, D. Ostojic, C. Rossi: Experimental tests on a multilevel converter for grid-connected photovoltaic sys-tems, 11th Workshop on Control and Modelling for Power Electronics, COMPEL. 17-20 Aug. 2008, pp. 1-7.

[13] J.H. Park, J.Y. Ahn, B.H. Cho, G.J. Yu: Dual-Module-Based Maximum Power Point Tracking Control of Photovoltaic Systems, IEEE Trans. on Ind. App., vol. 53, No. 4, June 2006, pp. 1036- 1047.

[14] G. Grandi, C. Rossi, G. Fantini: Modular Photovoltaic Generation Systems Based on a Dual-Module MPPT Algorithm, IEEE International Symposium on Industrial Electronics, IEEE-ISIE, Vigo (Spain), June 4-7, 2007.

[15] H. Stemmler and P. Guggenbach: Configurations of high-power voltage source inverter drives, in Proc. Power El. and App. Conf., 1993, vol.5, pp. 7-14.

[16] C. Rossi, D. Casadei, G. Grandi, A. Lega: Multilevel Operation and Input Power Balancing for a Dual Two-Level Inverter with Insulated DC Sources, IEEE Trans. on Industry Applications, vol. 44, No. 6, Nov/Dec 2008.

[17] M. Baiju, K. Mohapatra, R. Kanchan, K. Gopakumar: A dual two-level inverter scheme with common mode voltage elimination for an induction motor drive, IEEE Trans. on Power Electronics, vol. 19, No. 3, May 2004, pp. 794-805.

[18] F. Blaabjerg, R. Teodorescu, M. Liserre, A.V. Timbus: Overview of Control and Grid Synchronization for Distributed Power Generation Systems, IEEE Trans. on Industrial Electronics, vol. 53, no. 5, pp. 1398-1409, Oct. 2006.

[19] G. Grandi, D. Ostojic: Dual Inverter Space Vector Modulation with Power Balancing Capability, IEEE Region 8 Conference, EUROCON 2009, St. Petersburg, Russia, May 2009.